ELSEVIER

Contents lists available at ScienceDirect

# **Quaternary Science Reviews**

journal homepage: www.elsevier.com/locate/quascirev





# Climate, vegetation, and fire, during the last deglaciation in northwestern Amazonia

A. Blaus <sup>a</sup>, M.N. Nascimento <sup>b</sup>, L.C. Peterson <sup>c</sup>, C.N.H. McMichael <sup>a,b</sup>, M.B. Bush <sup>a,\*</sup>

- <sup>a</sup> Institute for Global Ecology, Florida Institute of Technology, Melbourne, FL, USA
- b Department of Ecosystem and Landscape Dynamics, Institute for Biodiversity and Ecosystem Dynamics, University of Amsterdam, Amsterdam, the Netherlands
- <sup>c</sup> Rosenstiel School of Marine and Atmospheric Science, University of Miami, Miami, FL, USA

#### ARTICLE INFO

Handling editor: Donatella Magri

Keywords:
Amazonia
Charcoal
Deglaciation
Heinrich event
Pollen
Last glacial maximum
XRF
Tropical forests

#### ABSTRACT

The magnitude of change in climatic conditions and vegetation response to the last deglaciation in various parts of tropical Amazonia is poorly understood and controversial. Analysis of a sediment core e.g. fossil pollen, X-ray Fluorescence (XRF) and charcoal from Lake Malachite on the Hill of Six Lakes in northwestern Brazil provided a deglacial history of climate, vegetation change and fire. Pollen revealed a forested landscape throughout, with shifts in composition that were driven by warming and changes in precipitation. The glacial cooling of c. 4-5 °C had brought species characteristic of cooler climates into the Amazon lowlands and was followed by an initial warming that began at least 19.5 thousand calibrated years before the present (cal kyr BP). Temperature oscillations and changes in precipitation between (18-14.6 cal kyr BP) associated with Heinrich Stadial 1 were observed as wet-dry-wet oscillations similar to some of the previous studies, and were evident in both pollen and XRF data. The pollen spectra were consistent that of a mesic forest before and after the peak of the Last Glacial Maximum. Cool-adapted taxa had previously been described from other cores from the Hill of Six Lakes, and persisted in low abundances until c. 14.1 cal kyr BP. No distinct response to the Atlantic Cold Reversal was evident in our proxy data. The early Holocene was marked by pollen, charcoal, and sedimentary changes that could reflect a peak drought stress on the forest. The large occurrence of charcoal indicating an increase in fires coincided with disturbance elements e.g. Cecropia and Alchornea, that could have been consistent with human disturbance of the forest at c. 10.2 cal kyr BP.

# 1. Introduction

Ice ages, also known as glacial periods, have had a profound effect on Earth's climate, geography, and ecosystems (Clark et al., 2012; Wang et al., 2017). Our knowledge of the effects of ice ages on lowland Amazonia comes from a limited number of studies often with low temporal resolution (Bush et al., 2004; Maslin and Burns, 2000; Van der Hammen and Absy, 1994). The Hill of Six Lakes (Ho6L) in northwestern Brazil is one of the very few locations to provide fossil pollen records from Amazonia that reflect conditions during the last ice age. Cores raised in 1991 provided long (>50,000 yr) fossil pollen records from three lakes (Pata, Verde, and Dragão, Fig. 1). The Lake Pata record was described by Colinvaux et al. (1996) and Bush et al. (2002) and a parallel core raised in that same drilling campaign was analyzed by D'Apolito et al. (2013). The Dragão and Verde records were described by Bush et al. (2004), and, taken together, these data revealed that a dry event

interrupted sediment accumulation on the Hill of Six Lakes between c. 35 cal kyr BP and 23 cal kyr BP. On either side of this event, the hill supported a forest that was a closed canopy system, but in which warm mesic elements such as Urticaceae/Moraceae and *Cecropia* were rare, while Myrtaceae, Melastomataceae, *Alchornea* and the cool elements, *Podocarpus, Hedyosmum, Weinmannia* and *Myrsine* were relatively abundant.

These findings were also crucial in the longstanding debate of the refugium theory (Haffer, 1969), which was believed to explain the unique biodiversity in the Amazon Basin. The H06L lay outside any refugium according to maps of Haffer (1969), but refugial boundaries were later moved to enclose it (Haffer and Prance, 2001). However, paleoecological data from the Ho6L refuted the refugial hypothesis (Bush and Oliveira, 2006; Colinvaux, 1998; Colinvaux et al., 1996) and did not show the reduction and fragmentation of forest cover.

A further coring of Lake Pata in 2009 provided a 7600-year long

E-mail address: mbush@fit.edu (M.B. Bush).

<sup>\*</sup> Corresponding author.

sediment record for chemical analyses (Cordeiro et al., 2011, Nogueira et al., 2021), and a detailed Holocene palynological history. This pollen record revealed the stability of vegetation around the lake throughout the mid and late Holocene (Nascimento et al., 2019).

Prior studies in lowland Amazonia indicated a cooling of as much as 4-5 °C during peak cold events within the glacial (Bush et al., 1990; Liu and Colinvaux, 1985). These estimates were affirmed by the initial studies of sediments from the Ho6L (Colinvaux et al., 1996). Evidence for glacial-aged cooling came from the presence of a suite of cold-adapted taxa, which included three distinct Podocarpaceae pollen types, Hedyosmum, Weinmannia and Myrsine before and after the Last Glacial Maximum (LGM; c. 26,000-20,000 cal BP). Indeed, these taxa are almost ubiquitous in glacial-aged records from Amazonia (Bush et al., 2004; Colinvaux et al., 1996; Ledru et al., 2001; Urrego et al., 2009). As these taxa are today largely restricted to elevations above c. 1500 m, their occurrence in the lowlands was interpreted to indicate a downslope migration of c. 1000-1200 m. During the glaciation, in addition to cooling, precipitation was reduced, and the extent and duration of dry periods within the last ice age are still actively debated (Bush and Silman, 2007; Colinvaux and Oliveira, 2000; Van der Hammen and Absy, 1994; Wang et al., 2017).

Isotopic data from a speleothem record in Central Amazonia suggested that for brief periods during the last glacial precipitation were reduced by as much as 58% relative to modern (Wang et al., 2017). Despite such strong apparent drying, <sup>13</sup>C isotopic data from the same speleothems showed that this was not enough to shift the vegetation toward a C4-dominated (i.e. grassland) system (Wang et al., 2017). Despite low atmospheric CO<sub>2</sub> concentrations, several factors probably contributed to the durability of the forest compared with modern systems. The first was that fire was extremely rare prior to human arrival

(Gosling et al., 2021), the second was that peak drying events were of relatively short duration as Amazonian precipitation was often linked to millennial-scale variance in Dansgaard-Oeschger cycles and Heinrich events (Zhang et al., 2017). Lastly, the net effect of the drying was mitigated by cooling that reduced some of the precipitation and, so far, all proxy records from central and western Amazonia have revealed a history of continuous forest cover throughout the last glacial cycle (Bush, 2017).

An emerging theme of paleoclimatic studies in the tropics over the last 20 years has been the importance of Atlantic sea-surface temperatures in forcing Heinrich Events (HEs) and Dansgaard-Oeschger (D-O) cycles. The major climatic perturbations caused by these irregular (pseudo-cyclic) events occurred at millennial scales and were especially evident during full glacial conditions in many settings (Cheng et al., 2013; Clark et al., 2012; Liu et al., 2018; Novello et al., 2017; Rodbell et al., 2022). These cycles were tentatively identified in fossil pollen sequences from southwestern Amazonia (Bush et al., 2004), and in the high Andes (Cheng et al., 2013; Groot et al., 2011; Rodbell et al., 2022). Northern Amazonian records, however, show either a less coherent signal in the late glacial (between c. 35 cal kyr BP and 17 cal kyr BP) than before (Mosblech et al., 2012) or a hiatus in deposition (Bush et al., 2004; Cheng et al., 2013; Colinvaux et al., 1996; Urrego et al., 2005; Wang et al., 2017). Hence, HE2 (c. 24 cal kyr BP) and HE3 (c. 29 cal kyr BP) are poorly represented in records from Amazonia. HE1 (c. 17 cal kyr BP) and HE0 (c. 12.5 cal kyr BP) are within the period when northernAmazonian speleothems and lakes can yield sediment records. As higher resolution records have come available it is clear that each Heinrich Stadial was composed of multiple Heinrich events (Hodell et al., 2017). Within Heinrich Stadial 1 (HS1; c. 18-14.5 cal kyr BP), Heinrich Event 1 (HE1) now appears to be driven by a major iceberg

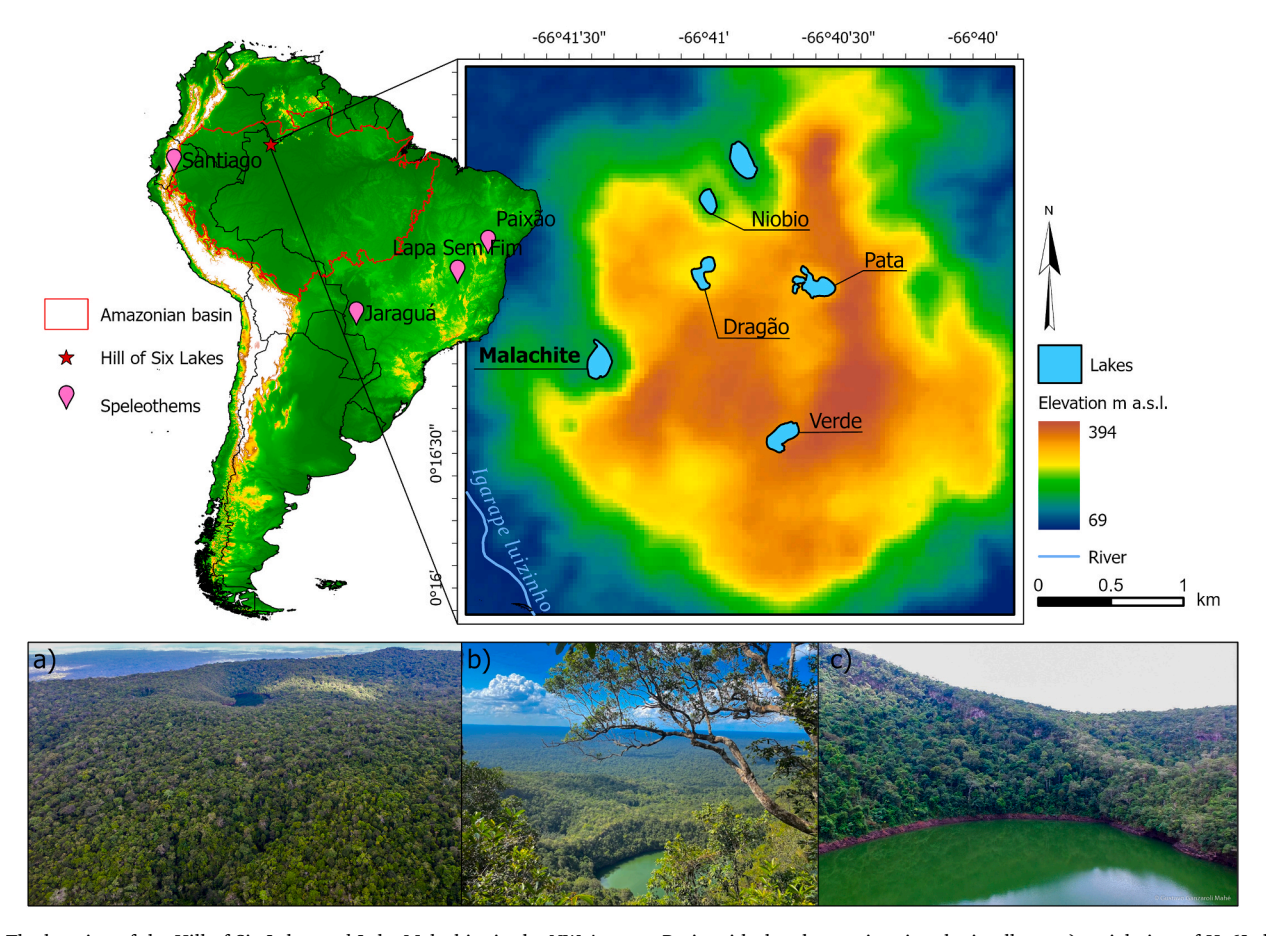


Fig. 1. The location of the Hill of Six Lakes and Lake Malachite in the NW Amazon Basin with the photos picturing the inselberg. a) aerial view of Ho6L. b) Lake Malachite from the trail to the top of the hill, and c) Lake Malachite. Photos a) and b) Gustavo Ganzaroli Mahé, and photo c) by Liany Pechar.

discharge at c. 16.2 cal kyr BP with a lesser peak at c. 15.1 cal kyr BP. A distinction is drawn between these iceberg discharges and the ensuing climatic repercussions that lasted for a few centuries, and the Heinrich1 Stadial, which is marked by Arctic cooling, Antarctic warming, and increasing atmospheric concentrations of CO<sub>2</sub> and CH<sub>4</sub>. Broecker and Putnam (2012) suggested that the stadial consisted of two substages with the divide being at c. 16.1 cal kyr BP. Analysis of speleothem data from Jaraguá Cave in southwestern Amazonia (Fig. 1) suggested a wet-dry-wet oscillation, i.e. three substages within HS1 with divisions at c. 17 and 16.1 cal kyr BP (Novello et al., 2017). This three-part oscillation also appears to be present in speleothem isotope data from Santiago (Mosblech et al., 2012), Lapa Sem and Fim and Paixão caves (Stríkis et al., 2018). The end of HE1 is generally taken to be between 15 and 14.5 cal kyr BP.

The transition to Holocene climates in Andean systems often included climatic oscillations such as the Antarctic Cold Reversal (ACR; c. 14.7–13 cal kyr BP) or HEO (c. 12.9–11.7 cal kyr BP), also known as the Younger Dryas event (Urrego et al., 2015; Van Der Hammen and Hooghiemstra, 1995). Although HEO was a wet event in northern Amazonia as the position of the Inter-Tropical Convergence Zone migrated southward (Deplazes et al., 2013; Zhang et al., 2017), it is not clearly defined closer to the equator (Raczka et al., 2018; Van Breukelen et al., 2008). In the northern Pantanal Bolivia, i.e. the southernmost fringe of Amazonia, diatom and X-ray fluorescence (XRF) data provided evidence of a wet Younger Dryas event and a vegetation transition from floodplain forest to seasonally flooded grasslands (Metcalfe et al., 2014; Whitney et al., 2011).

The deglacial warming is believed to have promoted the dispersal of humans into the Americas with people arriving in Amazonia by 13 cal kyr BP (Roosevelt, 2013). In paleoecological records, an increase in fire activity is a common signal of human presence between 10 and 8 cal kyr BP (Gosling et al., 2021). There is strong evidence that people were linked to the final extinction of the Pleistocene megafauna in the Andes, which seem to coincide with general megafaunal population extirpation (Bush et al., 2022; Pym et al., 2023; Raczka et al., 2019). In the dense lowland forests of Amazonia, a lack of fossil evidence makes it difficult to determine the geography and density of Pleistocene megafaunal populations, but it is likely that human arrival similarly adversely affected those animals that were present (Asevedo et al., 2021; de Fátima Rossetti et al., 2004; Guimaraes Jr et al., 2008; Janzen and Martin, 1982; Malhi et al., 2016).

While there is mounting evidence of climate change associated with D-O events in the Atlantic Ocean, it is not clear whether these fluctuations influenced forest composition in lowland Amazonia. Here, through fossil pollen, charcoal, and sediment chemistry analyses, we investigate the scale and timing of fire, vegetation and climate changes from the end of the LGM through Termination 1, i.e. the end of the last ice age, into the Holocene from Lake Malachite, Ho6L, in northern Amazonia. We assess whether deglacial climate and vegetation changes reflect Atlantic forcing, and weather early human influence on vegetation occurred at Lake Malachite in the Pleistocene-Holocene transition.

#### 2. Study area

Lake Malachite lies on the Hill of Six Lakes (Ho6L) at latitude 0.276139°N, longitude, 66.678612°W in Amazonas state in the northwestern part of Brazil (Fig. 1). The Ho6L is known as a Morro dos Seis Lagos biological reserve which is a part of Pico da Neblina National Park. In 2018, a coring campaign centered on two lakes that had not previously been cored on the Ho6L, Lakes Niobio and Malachite (Fig. 1). Lake Malachite, the subject of this paper, is the lowest-lying lake (ca. 180 m a. s.l) on the Ho6L, and it was expected that it might be less susceptible to groundwater variability than the lakes that lie on top of the inselberg, e. g., Pata (Bush et al., 2004). The inselberg is comprised of Cretaceous carbonatite and has been subjected to intense local weathering. A lateritic crust (ca. 200 m thick) rich in rare earth elements covers the

Cretaceous carbonatite (Cordeiro et al., 2011). Due to the geological uniqueness and abundance of rare earth elements, especially Niobium (Ni) and Titanium (Ti), the region of Ho6L has been in attention of minerologists and geochemists (Cordeiro et al., 2011; Giovannini et al., 2017, 2021).

Lake levels seem to be sensitive to precipitation as these lakes have previously been shown to be imperfectly sealed, dropping by several meters after a few days without rain (Bush et al., 2004). The average annual air temperature at the hill varies from 26 to 28°  $^{\circ}\text{C}$  and the mean annual precipitation in the region is around 2100 mm, with no pronounced dry season (Sombroek, 2001). The Ho6L should support moist tropical forest, but the very thin soils make this setting edaphically dry. The edaphic dryness leads to a small stature forest with a canopy at 8–15 m on the top of the hill and 25–30 m at the base of the Inselberg. Moss pollsters collected on the top of the Ho6L during a field season in 1991 revealed that the modern pollen inputs on the lakes on top of the hill were commonly dominated by Alchornea, Melastomataceae, Myrtaceae, Moraceae, and Salicaceae (Bush et al., 2004). There is no known history of occupation by humans, although the adjacent lowlands are part of the Balaio Indigenous Territory sparsely settled by different ethnic groups in Arawak and Tucano linguistic families (Farias, 2013).

#### 3. Materials and methods

In October 2018, c. 6 m-long sediment core was raised from the center of Lake Malachite from 7 m of water, using a Colinvaux-Vohnout piston corer (Colinvaux et al., 1999). The core was transported to the Florida Institute of Technology and stored at 4 °C. Due to the absence of plant macrofossils, twelve bulk sediment samples were dated using AMS radiocarbon <sup>14</sup>C from DirectAMS and the National Ocean Sciences Accelerator Mass Spectrometry (NOSAMS) facility at Woods Hole Oceanographic Institution. The age-depth model for the Lake Malachite sediment record was constructed using Bayesian statistics incorporated in the R software package "Bacon" (Blaauw and Christen, 2011). The IntCal20 calibration curve for the northern hemisphere was used to develop the model (Reimer et al., 2020). The age-depth model and sampling resolution were used to calculate the sediment accumulation rate, expressed in mm/year.

Based on the age-depth model, the topmost part of the core that covers 1.2 m and spans the LGM and deglacial periods were sampled for pollen analysis. The pollen analysis was performed following the standard preparation procedure (Faegri and Iversen, 1989). In total 58 samples in size of 0.5 cm<sup>3</sup> were analyzed for every second centimeter and Lycopodium clavatum spores were added to measure pollen concentration (Stockmarr, 1971). In each sample 300 pollen grains were identified and counted using an Axio Imager A2 photomicroscope at ×400 and ×630 magnifications. Pollen atlases (Colinvaux et al., 1999; Herrera and Urrego, 1996), and the database from Neotropical Paleoecology research group at Florida Institute of Technology (Bush and Weng, 2007) were used for pollen identification. In this region, Melastomataceae (mostly shrubs and small trees) produce pollen that tends to be smaller than Combretaceae (mostly vines and large trees) and do not have such distinct pores, but because the pollen morphotypes overlap they are often listed as a single type, Melastomataceae/Combretaceae. The majority of grains that we detected were Melastomataceae-type with very few that we assigned to Combretaceae. As only Melastomataceae (5 genera) but no Combretaceaae are documented in the Global Biodiversity Information Facility (GBIF.org) records from Ho6L, hereafter we interpret all pollen of this type as Melastomataceae. Similarly, Moraceae and Urticaceae have indistinguishable pollen, but they are reported here as Moraceae because we observed Brosimum (Moraceae), but no Urticaceae (other than Cecropia, which is reported separately), and there are no records of Urticaceae from the Ho6L in the GBIF database. Microscopic charcoal was counted on the pollen slides until the sum of pollen on each slide reached 300 grains and was expressed as the number of particles in relation to the pollen

#### concentration.

To study chemical parameters, we used an Avaatech X-ray fluorescence spectrometer (XRF) at the University of Miami, Department of Marine Geosciences to scan the core at 1 cm intervals. Due to lithological properties (dry sediment with an uneven surface), XRF were not initially scanned, and these parts were later re-scanned with the same methodology. To avoid data discrepancies related to XRF scanning on different occasions the elemental data were converted to z-scores (standard deviations from the mean) with means and standard deviations calculated separately for the two data-gathering sessions.

We performed a CONISS analysis, i.e., hierarchical cluster analysis on square root transformed (Bray Curtis dissimilarity) pollen data on all taxa, including aquatics (Grimm, 1987), to produce the pollen zones. We used the broken stick method (Bennett, 1996) to decide the number of significant zones (Supplement 1, Figs. S1–S2). Detrended correspondence analysis (DCA) (Hill and Gauch Jr, 1980) was performed on all taxa identified in the fossil pollen sequence. Axes 1 and 2 scores were plotted against time to determine the timings of significant vegetation change (Fig. 3). All statistical analyses and plotting were performed using the R software R-4.3.0 (R Development Core Team, 2019) and the packages "rioja" (Juggins, 2017), community ecology package "vegan" (Oksanen et al., 2019) and "ggplot2" (Wickham et al., 2016).

#### 4. Results

The upper 85 cm of the Lake Malachite sedimentary record represents the last c. 21 cal kyr BP (Table 1; Fig. 2). The youngest age yields ca 6 cal kyr BP at the top of the core based on the age-depth model. Ages marked with an \* at 60 cm and 85 cm depths were improbably young, treated as outliers, and not included in the age model (Table 1, Fig. 2). All other finite ages were included in the age model. Due to the improbable age and lithological properties of the sediment (changes in sediment texture and color) the depth at 85 cm is marked as the sedimentation hiatus. By default, the same accumulation rates were assumed for the model before and after the hiatus. The estimated hiatus starts around 31 cal kyr BP and spans to 21 cal kyr BP. Low sedimentation rates (0.005 mm/year) are recorded before and after the hiatus during the deglaciation and relatively higher increase was recorded in the early Holocene up to 0.5 mm/year (Fig. 2).

In total over 230 pollen taxa were recorded from the sediment record (Supplement 2), and 61 taxa occurred in excess of 5% abundance (Fig. 3). Of total taxa ca. 135 were trees and shrubs and 15 palms. We record 24 taxa in vines and lianas, 36 herbaceous taxa and 10 aquatic taxa. In terms of pollination, 214 taxa were animal pollinated, 22 wind

Table 1
Radiocarbon<sup>14</sup>C ages and calibrated ages using the Intcal 20 calibration curve (Reimer et al., 2020) from Lake Malachite, Brazil. All calibrated ages are rounded to the nearest 10 years.

DirectAMS code	Depth (cm)	Radiocarbon age		Calibrated ages	
		ВР	1 δ error	Median Intcal 20	2 Sigma range
OS-165224	7	6300	30	7220	7070-7350
OS-165225	15	8410	35	9310	8980-9550
OS-165226	25	8570	35	9540	9480-9600
OS-142571	33	8540	40	9520	9480-9550
D-AMS 46670	41	11,831	34	13,690	13,600–13,780
D-AMS 46671	60	11,377	46	13,250	13,170–13,330*
D-AMS 050515	73	15,418	60	18,750	18,390–18,860
OS-165227	85	13,650	65	16,490	16,280-16,740*
D-AMS 050514	90	29,461	198	33,490	32,220–34,220
D-AMS 46673	100	30,718	140	34,880	34,000–35,510

pollinated and 2 taxa were pollinated by both methods. The broken stick model indicated that the dataset has five significant zones present in the CONISS analysis (Supplement Figs. S1–S2) which we characterized below. The DCA of the fossil pollen data revealed relatively short gradient lengths, but samples belonging to the CONISS zones were largely segregated from one another (Fig. 4). The first two axes of DCA explained 31.7% of data variability. Every sample analyzed contained at least trace amounts of microscopic (10–40  $\mu m$ ) charcoal.

#### 4.1. Local zone Mal-1 (85-76 cm; 22-19.3 cal kyr BP)

Pollen concentrations were highly variable ranging from 2408 to 185,498 grains/cm³. Pollen assemblages were dominated by Melastomataceae (up to 21%) and Myrtaceae (up to 12%) with Arecaceae, Elaeocarpaceae, and Asteraceae showing some of their highest values of the record all but still occurring at < 5%. A large number of degraded pollen grains (3–10%) that might indicate harsh pollen preservation conditions or a substantial period when they lay on the surface before being washed into the lake were recorded in Mal-1 (Fig. 3). DCA showed that samples from the zone Mal-1 were located on the positive end of Axis 1 and were associated with cooler indicator taxa (*Podocarpus, Weinmannia, Ilex*) as well as Asteraceae, Elaeocarpaceae, Araliaceae, Malpighiaceae. The number of microscopic charcoal fragments found in Mal-1 samples ranged from 4 to 92 (Fig. 4). Sediment chemistry showed that Al, Si Ti and Fe all showed an initial decline, whereas Ca, Sr and Zr values increased in Mal-1 (Fig. 5).

#### 4.2. Local zone Mal-2 (76-62 cm; 19.3 to 15.4 cal kyr BP)

In general, Mal-2 has higher pollen concentrations than Mal-1, with up to 197,057 grains/cm<sup>3</sup>. Melastomataceae (44%) and Myrtaceae (28%) were more abundant than in Mal-1. Increases in *Cecropia*, *Mimosa-type*, and decreases of Arecaceae and the cool indicator taxa *Podocarpus*, *Weinmannia*, and *Myrsine* were recorded (Fig. 3). Mal-2 samples have positive scores on DCA Axis 1 and negative scores on Axis 2 and were associated with *Myrsine*, Melastomataceae, Myrtaceae, and Polygalaceae (Fig. 4). Low amounts of charcoal (ca 4 to 150 fragments/sample) and a decrease in degraded pollen grains, compared to Mal-1, were recorded in this zone. Rb, Sr, Zr, Ca, and Ti rose to maximum values in the zone at 16.6 cal kyr BP, followed by an abrupt decline, while Al and Si have broadly opposite trends (Fig. 5).

# 4.3. Local zone Mal-3 (62-36 cm; 15.4 to 10.3 cal kyr BP)

Zone Mal-3 has pollen concentrations up to c. 159,077 grains/cm<sup>3</sup> similar to Mal-2, with a trend of decreasing concentrations toward the Holocene. Zone Mal-3 was marked by increases in Moraceae and *Cecropia*, which constituted 31–71% of the total pollen sum as Melastomataceae, and Myrtaceae declined in abundance. *Podocarpus* disappeared at the beginning of this zone, but *Weinmannia*, *Hedyosmum* and *Myrsine* persisted at very low values. Moderate levels of microscopical charcoal were recorded in Mal-3 (ca. 20 to 200 fragments/sample) along with relatively high values (up to 5%) of degraded pollen grains (Fig. 3). Mal-3 samples occupied the central part of DCA plot but have positive values on Axis 1 (Fig. 4). Faster sedimentation between c. 15 and 14 cal kyr BP was reflected in decreased values of Ca, Si, and Ti/Ca, but the increases in Ti, Fe, Sr, Rb, Zr, Rb/Sr and Al/Si. Around 13 to 11 cal kyr BP. Ca showed high values, but Ti has its lowest values of the record (Fig. 5).

# 4.4. Local zone Mal-4 (36 to 18 cm; 10.3 to 9.3 cal kyr BP)

Zone Mal-4 lasted a relatively short period with strong changes noticeable in both vegetation and sedimentary data (Figs. 3 and 5). *Alchornea* reached 21%, while Melastomataceae showed a gradual decline from 14 to 4%. The first half of the zone saw a drop in Moraceae

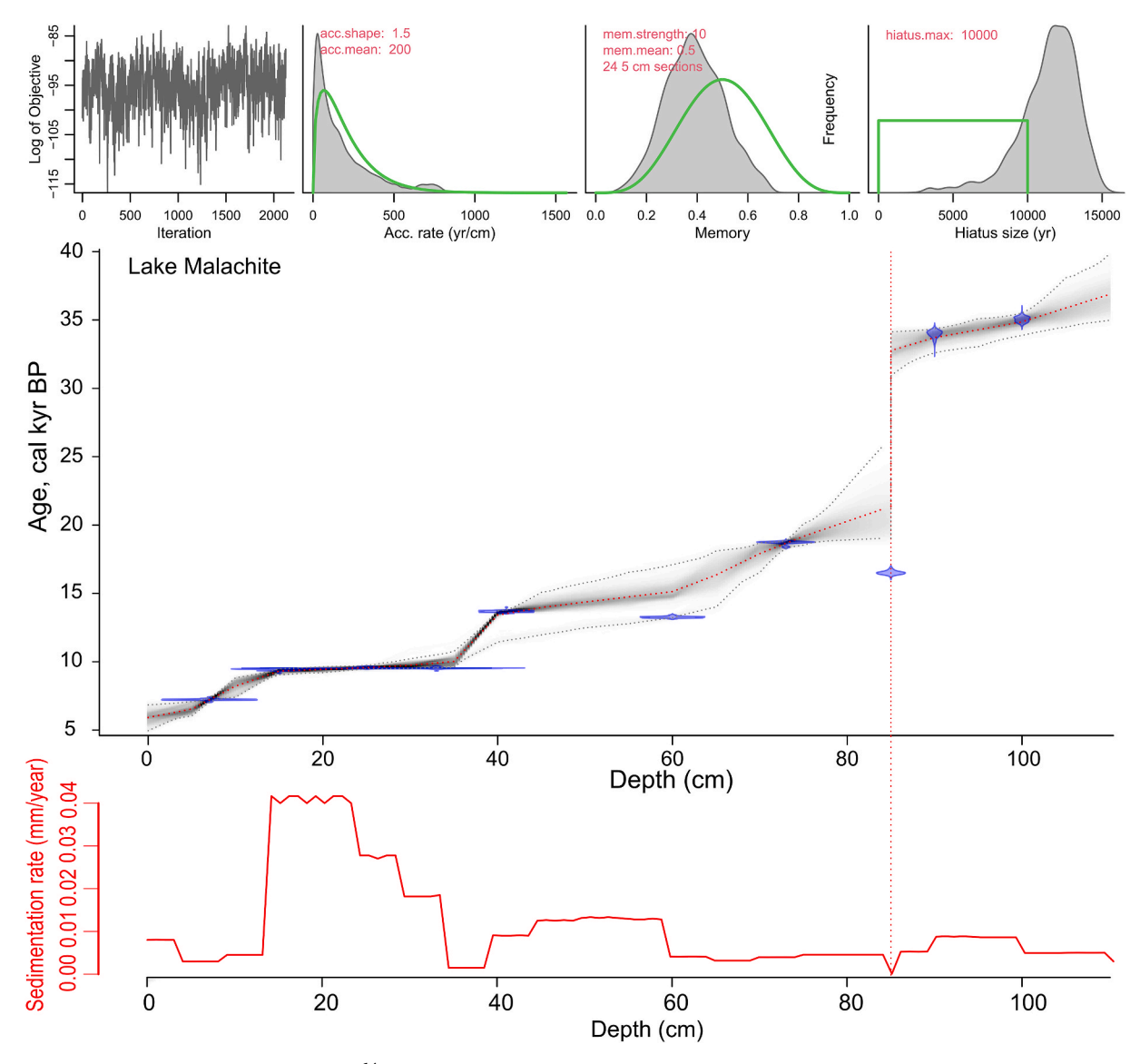


**Fig. 2.** Lake Malachite Age-depth model based on 11 <sup>14</sup>C AMS dates and developed using rBacon software program (Blaauw and Christen, 2011) and the IntCal 20 calibration (Reimer et al., 2020). The dotted red curve indicates weighted mean values of age depth model and vertical red line at the depth of 85 cm indicates an inferred hiatus in sedimentation. Details on AMS dates are summarized in Table 1. The red curve on the lower panel shows sediment accumulation rate expressed as mm/year.

(14–9%) followed by a rapid increase up to 28% by 9.3 cal kyr BP. Microcharcoal was more abundant compared with the previous zone with up to 570 fragments/sample (Fig. 3). Samples of Mal-4 samples has slightly negative scores on DCA Axis 1 and were associated with *Alchornea*, Moraceae, Anacardiaceae, Malvaceae, *Cassia* and Caesalpinioideae (Fig. 4). In the XRF data increases were recorded for Al, Fe, Fe/Ca, Rb/Sr, and Al/Si, as Rb, Sr, and Zr fell in abundance (Fig. 5).

#### 4.5. Local zone Mal-5 (18-0 cm; 9.3 to 6 cal kyr BP)

Mal-5 was dominated by Moraceae (up to 36%) and *Alchornea* (up to 19%) and a diversity of lowland forest pollen taxa, e.g. *Cassia*, Arecaceae, *Cecropia*, Caesalpinioidae, and Myrtaceae. Low pollen concentrations of ca. 40,000 grains/cm<sup>3</sup> were recorded in this zone. At the beginning of Mal-5 microcharcoal has high values (ca. 700 fragments/sample) which later decreased toward the mid-Holocene to 38 fragments/sample (Fig. 3). Samples representing Mal-5 were located on the negative end of Axis 1 on the DCA, and similar to Mal-4 were associated with *Alchornea*, Moraceae, Anacardiaceae, Malvaceae, and Cassia (Fig. 4). No XRF sediment chemistry was possible for this zone due to the

characteristics of the sediment (i.e. dry nature, granular texture).

### 5. Discussion

# 5.1. Environmental reconstruction

The sediment core raised from Lake Malachite provides a history of lowland Amazonian forest response to changing climate from the last glacial until the mid-Holocene. The very thin soils on the Ho6L means that the vegetation is a small-statured forest that is edaphically dry and cannot be described as typical rainforest for this elevation. Nevertheless, no evidence was found to support substantial loss of forest canopy at any time compared with the modern system. During the glacial period, the area around Lake Malachite supported a tropical forest that was a mixture of lowland taxa and cool-adapted taxa. The cool taxa, *Podocarpus, Myrsine* (ex *Rapanea*), *Hedyosmum, Ilex*, and *Weinmannia*, were a familiar group previously reported from lowland Amazonian glacial records (Anhuf et al., 2006; Bush et al., 2004; Ledru et al., 2001). These cool-adapted taxa are currently range restricted to altitudes above c. 1800 m, and thus they represented a considerable downslope migration

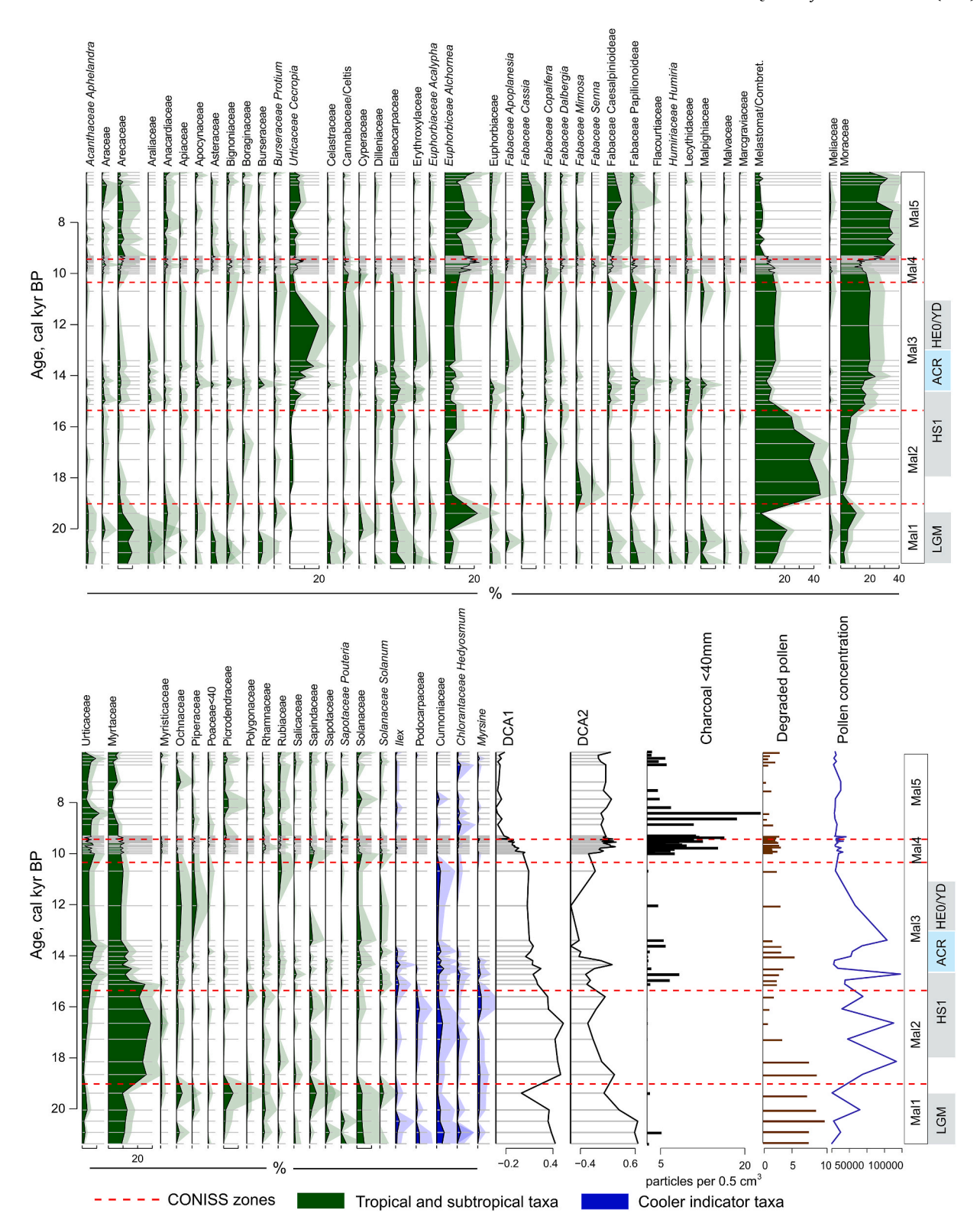


Fig. 3. Pollen diagram of taxa that occurred at >5% at least in one sample, and cool indicator species (blue) zoned using CONISS analysis (red, dashed lines). Also shown are DCA Axis 1 & 2 scores of pollen analysis, microscopic charcoal counts from pollen slides expressed in relation to pollen concentration, percentage of degraded grains, and pollen concentration.

of such taxa during the last ice age. Interspersed with these trees were typical lowland forest elements, e.g., Myrtaceae, Melastomataceae, Anacardiaceae, and Moraceae. This forest flora was very similar to that described from the full glacial of other lakes on the same hill (Bush and Silman, 2004; Colinvaux et al., 1996; D'Apolito et al., 2013), and is

interpreted as indicative of a cool, slightly drier-than-modern forest. Prior assessments suggested a c.  $4-5\,^{\circ}\mathrm{C}$  cooling would be needed for all the cold floral elements to have invaded the Hill of Six Lakes, and our data are consistent with that interpretation. A hiatus in which there was little sedimentation from c. 34 k to 22 cal kyr BP meant that, as with

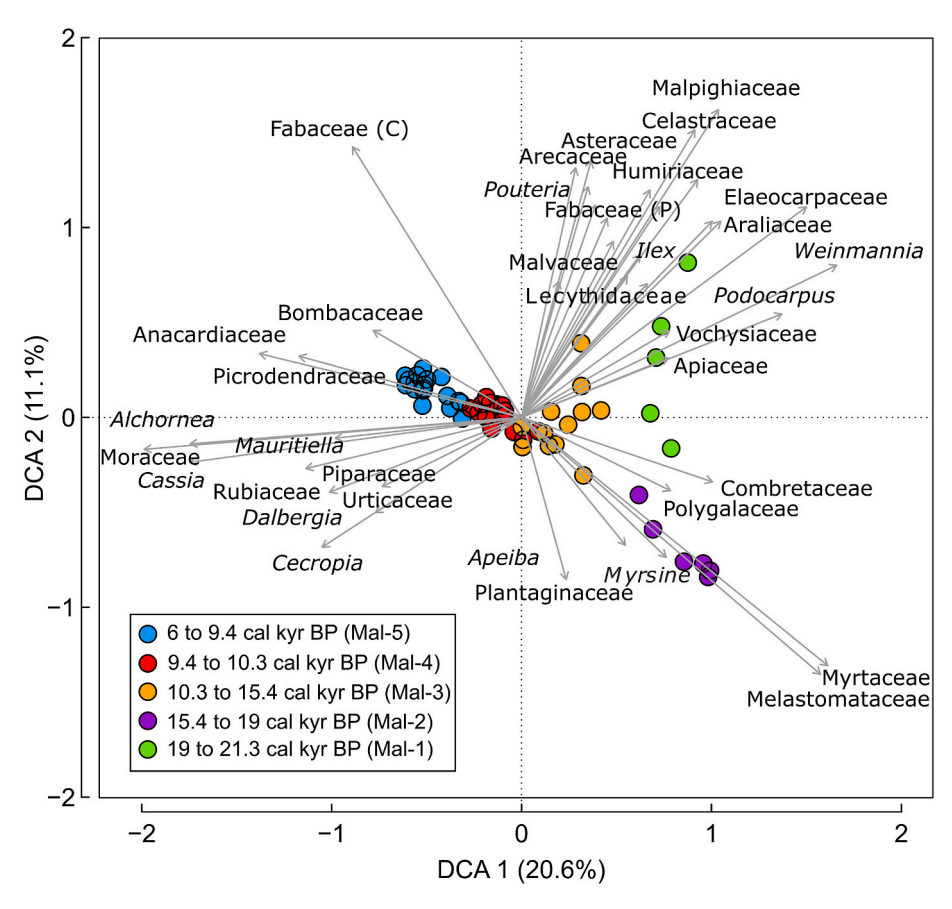


Fig. 4. Detrended correspondence analysis (DCA) Axis 1 vs 2 on pollen taxa. Only taxa with a significant correlation to Axes 1 or 2 are shown in the figure, with color-coded samples that mark the five CONISS-defined zones.

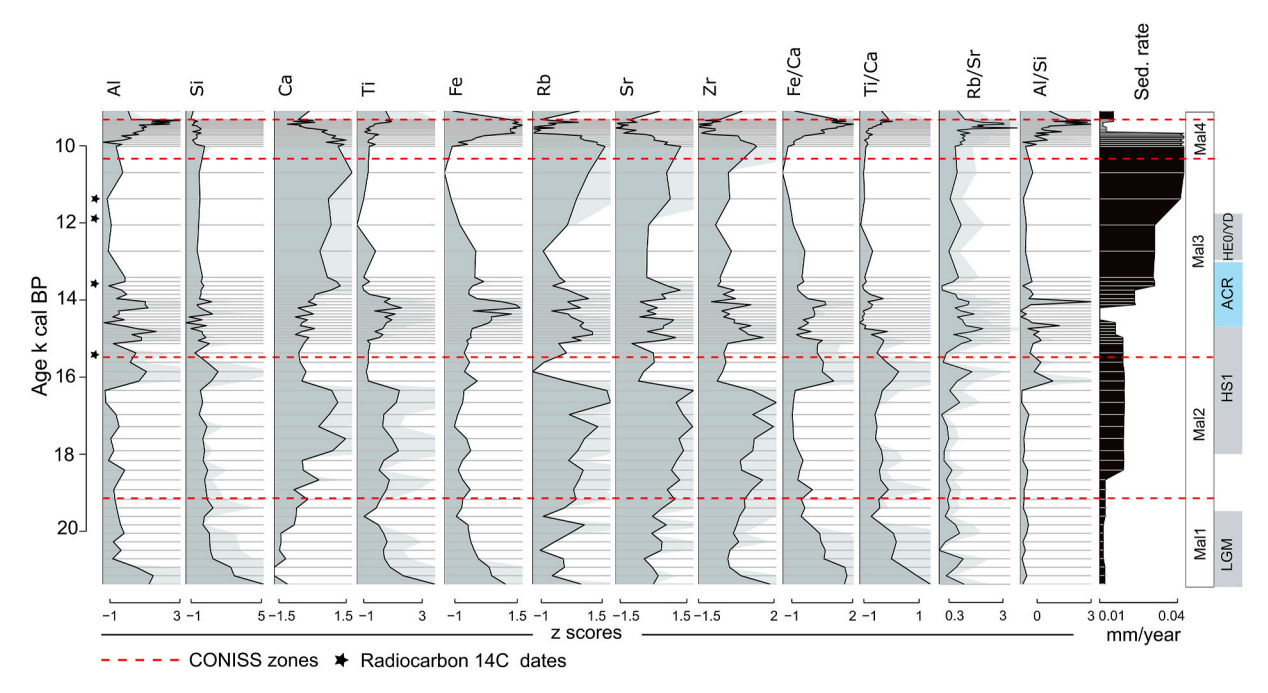


Fig. 5. Z-scores of major elements and element ratios derived from X-ray fluorescence analysis (XRF) on the sediments of Lake Malachite accompanied by the sediment accumulation rate (mm/year). Red, dashed lines indicate pollen zones from CONISS analysis and black stars represent <sup>14</sup>C dates for the particular section of the core.

other records from the Hill of Six Lakes, the full last glacial maximum was not documented from Lake Malachite (Bush et al., 2004; D'Apolito et al., 2013).

During the previous fieldwork in 1991, the rapid (2 m in 10 days) lowering of lake level suggested that the lakes on top of the inselberg were imperfectly hydrologically sealed and very sensitive to even short periods without precipitation (Bush et al., 2004). The location of Lake Malachite on the lower slopes of the inselberg might have been expected to have a water table nearer the level of the lake and therefore a more stable hydrology. Nonetheless, the presence of the LGM hiatus indicated that this lake was still perched above any permanent water table and apparently was as vulnerable as the other lakes to hydrological instability.

Sedimentation at Lake Malachite resumed in the late glacial at c. 22 cal kyr BP (local zone Mal-1), with a pollen spectra that still held a mixture of lowland forest, cool forest, and more open elements (Fig. 3 and Supplement Fig. S3). The indication of openness comes from the slightly elevated Asteraceae (6%) record, but as there is no accompanying peak of Poaceae (<2% throughout this record) the pollen was probably from Asteraceous shrubs or vines. The almost complete absence of charcoal in the pollen preparations suggests that fire was extremely rare in these ice-age forests.

#### 5.2. Did deglacial climate and vegetation changes reflect Atlantic forcing?

The deglacial trend of climate warming is captured in DCA Axis 1, where Moraceae and *Alchornea* are at the negative (warm) extreme of Axis 1, while Melastomataceae/Combretaceae, Myrtaceae, *Podocarpus*, cf *Weinmannia* are at the positive (cooler) extreme. The first strong sign of warming in the fossil pollen data is an increase in *Alchornea* pollen from c. 2% to c. 20% at c. 19.5 cal kyr BP (Fig. 3), along with the increase of Moraceae (up to 10%), Arecaceae and Anacardiaceae. These data suggest that conditions were both warm and wet. This evidence of a warm wet period between c. 22-20 cal kyr BP is consistent with other regional records (Mayle et al., 2000; Pym et al., 2023; Rozas-Davila et al., 2016; Seltzer et al., 2002; Whitney et al., 2011). The XRF data do not show the abrupt change seen in the pollen at c. 19.5–18.6 cal kyr BP, instead they show a gradual increase in terrigenous elements, e.g., Rb, Sr, and Zr, and to a lesser extent Ti, all of which are consistent with an increasingly wet climate causing erosion. After 18.6 cal kyr BP (Figs. 3)

and 6), the flora shifts to a forest rich in Melastomataceae (c. 40%) and Myrtaceae (c. 30%). In the study of 65 Amazonian lakes, no modern pollen sample included both Melastomataceae or Myrtaceae at >10% (Blaus et al., 2023), and in a study of >500 modern pollen samples from the Neotropics, only moss pollsters or pollen traps held such high abundances of either one, and no sample had such high abundances of both (Bush et al., 2020). The combination of such abundant Myrtaceae and Melastomataceae coupled with cool elements appeared to be a no-analog flora, but one that was cool and moist. This interpretation was consistent with trends observed in the regional speleothem data where the onset of HS1 was marked by a trend toward increasingly wet conditions between c. 18 and 16.6 cal kyr BP (Novello et al., 2017). Between 18.6 and 16.4 cal kyr BP both DCA Axis 1 and 2 (Fig. 3), which should reflect major changes in the pollen assemblages, are remarkably stable, suggesting that these changes in precipitation were insufficient to alter vegetation assemblages.

The XRF data from Lake Malachite suggested a general trend toward wetter conditions accelerating around 17.6 cal kyr BP as the inwash of Ca, Rb, Sr and Zr all increase. Generally, these elements represent weathering, and their release would likely be increased by both warming and wetting. Thus, there may be evidence for the climate becoming wetter at the onset of HS1 (c. 18 cal kyr BP) but not enough to alter the vegetation growing around the lake. The wet episodes within HS1 probably reflected North Atlantic cooling, weakening of Atlantic meridional overturning circulation (Henry et al., 2016) leading to a warming tropical Atlantic and the southward displacement of the ITCZ, which intensified the South American Summer Monsoon over the Amazon Basin (Deplazes et al., 2013; Stríkis et al., 2018; Wang et al., 2017; Zhang et al., 2017).

While the Malachite data suggest a general pattern of increasingly warm wet deglacial conditions interrupted by a dry event, producing a 3-stage early deglacial signal similar to that documented in Amazonian speleothems (Mosblech et al., 2012; Novello et al., 2019; Stríkis et al., 2018). Although the dating of these events is not quite aligned, though generally within dating error, the disparity is probably explained through a combination of very slow sedimentation at Lake Malachite and the usage of less precise <sup>14</sup>C-based chronology compared with U/Th-dated speleothems. Therefore, we would argue that the absolute ages reflected in the speleothems are probably the most accurate, but the Malachite data provide additional insights into the ecological effects of

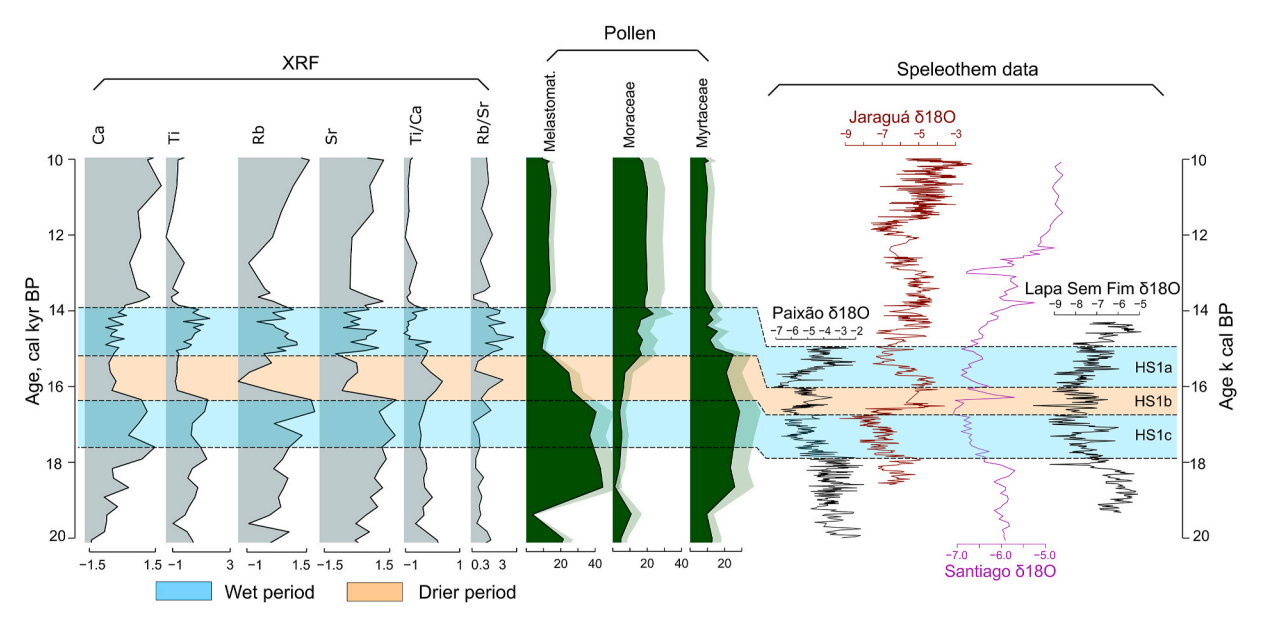


Fig. 6. Selected XRF data and pollen taxa from the Lake Malachite record are shown in relation to speleothem data (Fig. 1) from Caves Paixão and Lapa Sem Fim (Stríkis et al., 2018), Santiago Cave (Mosblech et al., 2012) and Jaraguá Cave (Novello et al., 2019). The timing of the wet-dry-wet oscillation in relatively well-dated speleothem records are mirrored by changes in the Malachite data, though the temporal offset is within the margin of error for the Malachite dataset.

the observed climatic changes. Our data shows only a weak response to the onset of HE1. Consequently, HS1c is only weakly differentiated from a longer climatic trend. The transition from HS1c and HS1b, which occurs c. 16.7 cal kyr BP in the speleothem records (Fig. 6) appears to influence vegetation between c. 16.7 and 16.4 (reflecting our sampling interval). That transition is caught more precisely in the higher-resolution XRF data at c. 16.4 cal kyr BP.

The ecological effects of the climate change observed at c. 16.4 cal kyr BP resulted in a marked transition in the appearance and chemistry of the sediment. The surface texture of the split core was noticeably rough between 40 and 60 cm depth, which caused an initial problem with the XRF scanning. A subsequent session in which extra attention was paid to scraping a cover slip across to improve contact between the core and the plastic film used to cover its surface for XRF measurements allowed data to be gathered. We recognized that the additional smoothing of the surface could have altered the XRF readings. Indeed, the readings from this core section looked to be quite different from the adjacent ones, but we considered it likely that the differences genuinely reflected altered chemistry, probably as the lake briefly shallowed and the mudwater interface became normoxic. Between 16.4 and 15.0 cal kyr BP terrigenous elements declined abruptly in their abundance as sedimentation rates fell from c. 0.013 mm per vr to 0.009 mm per vr (Fig. 6). These data were consistent with dry conditions reducing erosion and shallowing the lake. The flora at Lake Malachite did not exhibit a strong change in response to this drying but it was probably reflected in the declining abundance of Melastomataceae and a slight increase in wetland herbs in the Polygonaceae (Fig. 3). Six species of Melastomataceae have been documented on the Ho6L (Supplement 1 Table S1), five of which are described as needing wet forest environments. Similarly, seven species in Myrtaceae (1 endemic to the hill) have been documented, six of which are characteristic of wet forests (Supplementary Table 1). For the most part, the ecological tolerance of these species is unknown and clearly all are tolerant of modern edaphically dry conditions. It is very likely that the observed increases and decreases in pollen abundance in these lowland taxa represent relative changes in population size as opposed to colonization and extinctions.

The return of wetter conditions associated with HS 1a occurs at c. at 16 cal kyr BP in the speleothem records but does not begin until c. 15.2 cal kyr BP in the Malachite record when there is an increase in Ti and Rb/Sr, a proxy for coarser grain size (Plimer and Elliott, 1979). This increase in terrigenous elements is consistent with a warm, wet event that lasted until c. 14.1 cal kyr BP. The pollen data also reflect this transition as Myrtaceae decline in abundance while both common, e.g. Moraceae, Cecropia, Euphorbiaceae, Alchornea, and rarer components, e. g. Arecaceae, Araliaceae, Fabaceae, Elaeocarpaceae and Lecythidaceae, increase. About 14 cal kyr BP the cool-adapted taxa such as Podocarpus, Weinmannia and Hedyosmum, disappear from the Malachite record; an observation which is consistent with the other records from the Ho6L (Bush et al., 2004). We interpret this transition to be part of progressive warming.

Overall, according to our chronology, between c. 18 and 14.1 cal kyr BP there is evidence of a three-stage wet-dry-wet series of climate events (Fig. 3), with transitions at c. 16.4 and 15 cal kyr BP. Recognizing some well-known flat spots in the <sup>14</sup>C record around 15 cal kyr BP (Hodell et al., 2017), and the very slow rate of sedimentation at Lake Malachite, which adds uncertainty to chronologies, the timing of inferred events at Malachite is in broad agreement with those obtained from Amazonian and nearby speleothems (Novello et al., 2017).

# 5.3. Is there a human signal at Lake Malachite in the Pleistocene-Holocene transition?

Archaeological data are broadly lacking from this part of Amazonia although it has been suggested as a hub of domestication for *Theobroma grandiflorum* (*Cupuaçu*) (Colli-Silva et al., 2023). At least trace amounts of fine charcoal were seen on almost all the pollen slides, but the amount

of charcoal detected does not correlate clearly with inferred warming or drying. The period with the least charcoal is between c. 18 and 15 cal kyr BP. The occurrence of charcoal in the pollen slides increases between c 15 and 14 cal kyr BP, which is somewhat surprising given that this is overall a wetter interval than the preceding millennium (Fig. 6). The charcoal particles that we observed are <40  $\mu m$  and are a) rare and b) capable of long-distance dispersal. We do not infer that these fires occurred on the Ho6L but rather represent occasional regional fires. Although the rarity of fire in Amazonia in the absence of humans is well known (Gosling et al., 2021), the combination of the extirpation of the cool-adapted flora, increasing aridity and temperature suggests that the period from 15 to 14 cal kyr BP is one in which periodic drought interrupts an overall wet event (Nepstad et al., 2004), likley creating suitable conditions for natural fire. Additionally, humans cannot be excluded as a potential source of the fires.

The last major change in both the records of pollen and XRF data indicates a marked increase in precipitation around 10.2 cal kyr BP in what appears to be an instantaneous deposition of c. 18 cm of sediment. This input coincides with the largest sustained occurrence of charcoal in the core and an increase in the disturbance elements *Cecropia* and *Alchornea*. It is unclear whether the charcoal that we document at c. 10.2 cal kyr BP is the product of increased seasonality and peak Holocene temperatures (Van Breukelen et al., 2008) or if it is indicative of people exploiting this section of the Rio Negro in the early Holocene. The other records from Ho6L (Bush et al., 2004) do not show this same acceleration of sedimentation c. 10.2 cal kyr BP, but the watershed of Malachite is larger, and its position on the side of the hill could have allowed more soil inwash.

If the fires and erosion at c. 10.2 cal kyr BP were caused by human activity, such an apparently local signature, e.g., increased sedimentation rate and vegetation change, suggest that the occupation may have been close to the lake, perhaps at the base of the Ho6L beside the adjacent river Igarape Laizinho. Charcoal inputs remained elevated in the remaining Holocene samples, suggesting that if this was caused by people, they continued to be active in the forest. The earliest prior record of forest fires possibly ascribed to humans from this region was charcoal recorded in the soils of sites along the Rio Negro c. 7.16 cal kyr BP (Sanford Jr et al., 1985). Although, at the time, the authors of that study did not ascribe charcoal to human activity, and perhaps revisiting those records with more modern understanding would suggest the probability that those charcoal fragments represented human occupation. Whatever its cause, after this erosive event, as conditions probably became wetter and less seasonal (Legendre, 2019; Mosblech et al., 2012; Novello et al., 2019; Stríkis et al., 2018), the modern forest that is rich in Moraceae, Alchornea, Cecropia, Cassia and other Caesalpinioideae, formed.

### **Conclusions**

We add to the evidence that the region of Hill of Six Lakes remained forested throughout the deglaciation with compositional changes of taxa in response to warming and changing precipitation. After the LGM the vegetation on Hill of Six Lakes was mostly composed of Melastomataceae, and Myrtaceae, with a mixture of mesic elements and taxa associated with cooler climates, e.g., Podocarpus, Ilex, Myrsine, and Weinmannia. The changes in pollen spectra that followed reflected a wetdry-wet oscillation during HS1, with the dry period probably marking the peak of HE1, emphasizing that Atlantic sea-surface temperatures were playing an important role in shaping Amazonian climate and vegetation. The modern vegetation established gradually during the deglacial, with several different no-analog communities forming before the warming caused the local extirpation of cool-tolerant species about 14 cal kyr BP. A forest comparable to modern recognizably established only about 10.2 cal kyr BP. A new finding for this study was the possibility that people were occupying the upper Rio Negro at 10.2 cal kyr BP and influencing the vegetation near the base of the Hill of Six Lakes.

#### **Author contributions**

AB and MB conceived the ideas and wrote the manuscript with the contributions of all other authors. LP was responsible for XRF analysis. MN participated in Lake Malachite sediment core collection. AB did data gathering and analysis and generated all the figures. All authors contributed to data interpretation and MB and CM assisted with editing the manuscript.

#### Declaration of competing interest

The authors declare that they have no known competing financial interests or personal relationships that could have appeared to influence the work reported in this paper.

#### Data availability

Data will be made available on request.

### Acknowledgments

We acknowledge our colleagues and members of the indigenous Tucano community who participated in the fieldwork at Hill of Six Lakes. This work was supported by the NSF grant GR232452 to MBB, and a National Geographic Society Waitt Award to MNN.

#### Appendix A. Supplementary data

Supplementary data to this article can be found online at https://doi.org/10.1016/j.quascirev.2024.108662.

#### References

- Anhuf, D., Ledru, M.P., Behling, H., Da Cruz, F.W., Cordeiro, R.C., Van der Hammen, T., Karmann, I., Marengo, J.A., De Oliveira, P.E., Pessenda, L., Siffedine, A., Albuquerque, A.L., Da Silva Dias, P.L., 2006. Paleo-environmental change in amazonian and African rainforest during the LGM. Palaeogeogr. Palaeoclimatol. Palaeoecol. 239, 510–527.
- Asevedo, L., Ranzi, A., Kalliola, R., Pärssinen, M., Ruokolainen, K., Cozzuol, M.A., do Nascimento, E.R., Negri, F.R., Souza-Filho, J.P., Cherkinsky, A., 2021. Isotopic paleoecology (δ13C, δ18O) of late Quaternary herbivorous mammal assemblages from southwestern Amazon. Quat. Sci. Rev. 251, 106700.
- Bennett, K.D., 1996. Determination of the number of zones in a biostratigraphical sequence. New Phytol. 132, 155–170.
- Blaauw, M., Christen, J.A., 2011. Flexible paleoclimate age-depth models using an autoregressive gamma process. Bayesian Anal 6, 457–474.
- Blaus, A., McMichael, C., Raczka, M., Herrick, C., Palace, M., Witteveen, N., Nascimento, M., Bush, M., 2023. Amazonian pollen assemblages reflect biogeographic gradients and forest cover. J. Biogeogr. 50, 1926–1938.
- Broecker, W., Putnam, A.E., 2012. How did the hydrologic cycle respond to the twophase mystery interval? Quat. Sci. Rev. 57, 17–25.
- Bush, M., Miller, M., De Oliveira, P., Colinvaux, P., 2002. Orbital forcing signal in sediments of two Amazonian lakes. Journal of Paleolimnology 27, 341–352.
- Bush, M.B., Oliveira, P.E.d., 2006. The rise and fall of the Refugial Hypothesis of Amazonian speciation: a paleoecological perspective. Biota Neotropica 6.
- Bush, M., Rozas-Davila, A., Raczka, M., Nascimento, M., Valencia, B., Sales, R., McMichael, C., Gosling, W., 2022. A palaeoecological perspective on the transformation of the tropical Andes by early human activity. Philosophical Transactions of the Royal Society B 377, 20200497.
- Bush, M.B., 2017. The resilience of Amazonian forests. Nature 541, 167–168.
   Bush, M.B., Colinvaux, P.A., Wiemann, M.C., Piperno, D.R., Liu, K.-B., 1990. Late Pleistocene temperature depression and vegetation change in Ecuadorian Amazonia. Ouat. Res. 34, 330–345.
- Bush, M.B., Correa-Metrio, A., van Woesik, R., Collins, A., Hanselman, J., Martinez, P., McMichael, C.N.H., 2020. Modern pollen assemblages of the Neotropics. J. Biogeogr. 48, 231–241.
- Bush, M.B., De Oliveira, P.E., Colinvaux, P.A., Miller, M.C., Moreno, J.E., 2004. Amazonian paleoecological histories: one hill, three watersheds. Palaeogeogr. Palaeoclimatol. Palaeoecol. 214, 359–393.
- Bush, M.B., Silman, M.R., 2004. Observations on late Pleistocene cooling and precipitation in the lowland Neotropics. J. Quat. Sci. 19, 677–684.
- Bush, M.B., Silman, M.R., 2007. Amazonian exploitation revisited: ecological asymmetry and the policy pendulum. Front. Ecol. Environ. 5, 457–465.
- Bush, M.B., Weng, C., 2007. Introducing a New (Freeware) Tool for Palynology. Wiley Online Library, pp. 377–380.

- Cheng, H., Sinha, A., Cruz, F.W., Wang, X., Edwards, R.L., d'Horta, F.M., Ribas, C.C., Vuille, M., Stott, L.D., Auler, A.S., 2013. Climate change patterns in Amazonia and biodiversity. Nat. Commun. 4, 1411.
- Clark, P.U., Shakun, J.D., Baker, P.A., Bartlein, P.J., Brewer, S., Brook, E., Carlson, A.E., Cheng, H., Kaufman, D.S., Liu, Z., 2012. Global climate evolution during the last deglaciation. Proc. Natl. Acad. Sci. USA 109, E1134–E1142.
- Colinvaux, P., 1998. A new vicariance model for Amazonian endemics. Global Ecology & Biogeography Letters 7, 95–96.
- Colinvaux, P., De Oliveira, P.E., Moreno, E., 1999. Amazon Pollen Manual and Atlas. Taylor & Francis.
- Colinvaux, P.A., De Oliveira, P.E., Moreno, J.E., Miller, M.C., Bush, M.B., 1996. A long pollen record from lowland Amazonia: forest and cooling in glacial times. Science 274, 85–88.
- Colinvaux, P.A., Oliveira, P.E.D., 2000. Palaeoecology and climate of the Amazon basin during the last glacial cycle. J. Quat. Sci.: Published for the Quaternary Research Association 15, 347–356.
- Colli-Silva, M., Richardson, J.E., Neves, E.G., Watling, J., Figueira, A., Pirani, J.R., 2023.Domestication of the Amazonian fruit tree cupuaçu may have stretched over the past 8000 years. Communications Earth & Environment 4, 401.
- Cordeiro, R., Turcq, B., Sifeddine, A., Lacerda, L.D.d., Silva Filho, E., Gueiros, B., Potty, Y., Santelli, R., Pádua, E., Patchinelam, S., 2011. Biogeochemical indicators of environmental changes from 50 Ka to 10 Ka in a humid region of the Brazilian Amazon. Palaeogeogr. Palaeoclimatol. Palaeoecol. 299, 426–436.
- D'Apolito, C., Absy, M.L., Latrubesse, E.M., 2013. The Hill of Six Lakes revisited: new data and re-evaluation of a key Pleistocene Amazon site. Quat. Sci. Rev. 76, 140–155
- de Fátima Rossetti, D., de Toledo, P.M., Moraes-Santos, H.M., de Araújo Santos, A.E.d., 2004. Reconstructing habitats in central Amazonia using megafauna, sedimentology, radiocarbon, and isotope analyses. Quat. Res. 61, 289–300.
- Deplazes, G., Lückge, A., Peterson, L.C., Timmermann, A., Hamann, Y., Hughen, K.A., Röhl, U., Laj, C., Cane, M.A., Sigman, D.M., 2013. Links between tropical rainfall and North Atlantic climate during the last glacial period. Nat. Geosci. 6, 213–217.
- Faegri, K., Iversen, J., 1989. Textbook of Pollen Analysis. John Wiley & Sons, Chichester. Farias, E., 2013. Terras indígenas da Amazônia são alvos de pesquisas sobre terras raras. Amazônia Real (in Portuguese). (Accessed 30 November 2023).
- Giovannini, A.L., Neto, A.C.B., Porto, C.G., Pereira, V.P., Takehara, L., Barbanson, L., Bastos, P.H., 2017. Mineralogy and geochemistry of laterites from the Morro dos Seis Lagos Nb (Ti, REE) deposit (Amazonas, Brazil). Ore Geol. Rev. 88, 461–480.
- Giovannini, A.L., Neto, A.C.B., Porto, C.G., Takehara, L., Pereira, V.P., Bidone, M.H., 2021. REE mineralization (primary, supergene and sedimentary) associated to the Morro dos Seis Lagos Nb (REE, Ti) deposit (Amazonas, Brazil). Ore Geol. Rev. 137, 104308.
- Gosling, W.D., Maezumi, S.Y., Heijink, B.M., Nascimento, M.N., Raczka, M.F., van der Sande, M.T., Bush, M.B., McMichael, C.N., 2021. Scarce fire activity in north and north-western Amazonian forests during the last 10,000 years. Plant Ecol. Divers. 14, 143–156.
- Grimm, E.C., 1987. CONISS: a FORTRAN 77 program for stratigraphically constrained cluster analysis by the method of incremental sum of squares. Comput. Geosci. 13, 13–25
- Groot, M., Bogotá, R., Lourens, L., Hooghiemstra, H., Vriend, M., Berrio, J., Tuenter, E., Van der Plicht, J., Van Geel, B., Ziegler, M., 2011. Ultra-high resolution pollen record from the northern Andes reveals rapid shifts in montane climates within the last two glacial cycles. Clim. Past 7, 299–316.
- Guimaraes Jr, P.R., Galetti, M., Jordano, P., 2008. Seed dispersal anachronisms: rethinking the fruits extinct megafauna ate. PLoS One 3, e1745.
- Haffer, J., 1969. Speciation in Amazonian Forest Birds: most species probably originated in forest refuges during dry climatic periods. Science 165, 131–137.
- Haffer, J., Prance, G.T., 2001. Climatic forcing of evolution in Amazonia during the Cenozoic: on the refuge theory of biotic differentiation. Amazoniana: Limnologia et Oecologia Regionalis Systematis Fluminis Amazonas 16, 579–607.
- Henry, L., McManus, J., Curry, W., Roberts, N., Piotrowski, A., Keigwin, L., 2016. North Atlantic ocean circulation and abrupt climate change during the last glaciation. Science 353, 470–474.
- Herrera, L., Urrego, L., 1996. Atlas de polen de Plantas Útiles y Cultivables de la Amazonia Colombiana. Estudios en la Amazonía Colombiana, Tropenbos. ISBN 958-95378-7-1.
- Hill, M.O., Gauch Jr, H.G., 1980. Detrended correspondence analysis: an improved ordination technique. Vegetatio 42, 47–58.
- Hodell, D.A., Nicholl, J.A., Bontognali, T.R., Danino, S., Dorador, J., Dowdeswell, J.A., Einsle, J., Kuhlmann, H., Martrat, B., Mleneck-Vautravers, M.J., 2017. Anatomy of Heinrich Layer 1 and its role in the last deglaciation. Paleoceanography 32, 284–303
- Janzen, D.H., Martin, P.S., 1982. Neotropical anachronisms: the fruits the gomphotheres ate. Science 215, 19–27.
- Juggins, S., 2017. Rioja: analysis of Quaternary science data. R package version (0.9-15.1.
- Ledru, M.-P., Cordeiro, R.C., Dominguez, J.M.L., Martin, L., Mourguiart, P., Sifeddine, A., Turcq, B., 2001. Late-glacial cooling in Amazonia inferred from pollen at Lagoa do Caçó, northern Brazil. Quat. Res. 55, 47–56.
- Legendre, P., 2019. A temporal beta-diversity index to identify sites that have changed in exceptional ways in space-time surveys. Ecol. Evol. 9, 3500–3514.
- Liu, D., Wang, Y., Cheng, H., Edwards, R., Kong, X., Chen, S., Liu, S., 2018. Contrasting patterns in abrupt Asian summer monsoon changes in the last glacial period and the Holocene. Paleoceanogr. Paleoclimatol. 33, 214–226.
- Liu, K.-b., Colinvaux, P., 1985. Forest changes in the Amazon Basin during the last glacial maximum. Nature 318, 556–557.

- Malhi, Y., Doughty, C.E., Galetti, M., Smith, F.A., Svenning, J.-C., Terborgh, J.W., 2016.
  Megafauna and ecosystem function from the Pleistocene to the Anthropocene. Proc. Natl. Acad. Sci. USA 113, 838–846.
- Maslin, M.A., Burns, S.J., 2000. Reconstruction of the Amazon Basin effective moisture availability over the past 14,000 years. Science 290, 2285–2287.
- Mayle, F.E., Burbridge, R., Killeen, T.J., 2000. Millennial-scale dynamics of southern Amazonian rain forests. Science 290, 2291–2294.
- Metcalfe, S.E., Whitney, B.S., Fitzpatrick, K.A., Mayle, F.E., Loader, N.J., Street-Perrott, F.A., Mann, D.G., 2014. Hydrology and climatology at Laguna La Gaiba, lowland Bolivia: complex responses to climatic forcings over the last 25 000 years. J. Ouat. Sci. 29, 289–300.
- Mosblech, N.A., Bush, M.B., Gosling, W.D., Hodell, D., Thomas, L., Van Calsteren, P., Correa-Metrio, A., Valencia, B.G., Curtis, J., Van Woesik, R., 2012. North Atlantic forcing of Amazonian precipitation during the last ice age. Nat. Geosci. 5, 817–820.
- Nascimento, M.N., Martins, G.S., Cordeiro, R.C., Turcq, B., Moreira, L.S., Bush, M.B., 2019. Vegetation response to climatic changes in western Amazonia over the last 7,600 years. Journal of Biogeography 46, 2389–2406.
- Nepstad, D., Lefebvre, P., Lopes da Silva, U., Tomasella, J., Schlesinger, P., Solórzano, L., Moutinho, P., Ray, D., Guerreira Benito, J., 2004. Amazon drought and its implications for forest flammability and tree growth: a basin-wide analysis. Global Change Biol. 10, 704–717.
- Nogueira, J., Evangelista, H., Valeriano, C.d.M., Sifeddine, A., Neto, C., Vaz, G., Moreira, L.S., Cordeiro, R.C., Turcq, B., Aniceto, K.C., 2021. Dust arriving in the Amazon basin over the past 7,500 years came from diverse sources. Communications Earth & Environment 2, 5.
- Novello, V.F., Cruz, F.W., McGlue, M.M., Wong, C.I., Ward, B.M., Vuille, M., Santos, R.A., Jaqueto, P., Pessenda, L.C., Atorre, T., 2019. Vegetation and environmental changes in tropical South America from the last glacial to the Holocene documented by multiple cave sediment proxies. Earth Planet Sci. Lett. 524, 115717.
- Novello, V.F., Cruz, F.W., Vuille, M., Stríkis, N.M., Edwards, R.L., Cheng, H., Emerick, S., De Paula, M.S., Li, X., Barreto, E.d.S., 2017. A high-resolution history of the South American monsoon from last glacial maximum to the Holocene. Sci. Rep. 7, 44267.
- Oksanen, J., Blanchet, F.G., Friendly, M., Kindt, R., Legendre, P., McGlinn, D., Minchin, P.R., O'hara, R., Simpson, G.L., Solymos, P., 2019. Package 'vegan'. Community Ecology Package, Version 2(0), pp. 321–326.
- Plimer, I., Elliott, S., 1979. The use of Rb/Sr ratios as a guide to mineralization. J. Geochem. Explor. 12, 21–34.
- Pym, F.C., Franco-Gaviria, F., Espinoza, I.G., Urrego, D.H., 2023. The timing and ecological consequences of Pleistocene megafaunal decline in the eastern Andes of Colombia. Ouat. Res. 1–17.
- Raczka, M.F., Bush, M.B., De Oliveira, P.E., 2018. The collapse of megafaunal populations in southeastern Brazil. Ouat. Res. 89, 103–118.
- Raczka, M.F., Mosblech, N., Giosan, L., Valencia, B.G., Folcik, A., Kingston, M., Baskin, S., Bush, M., 2019. A human role in Andean megafaunal extinction? Quat. Sci. Rev. 205, 154–165.
- R Development Core Team, 2019. R: A Language and Environment for Statistical Computing. R Foundation for Statistical Computing.
- Reimer, P.J., Austin, W.E., Bard, E., Bayliss, A., Blackwell, P.G., Ramsey, C.B., Butzin, M., Cheng, H., Edwards, R.L., Friedrich, M., 2020. The IntCal20 Northern Hemisphere radiocarbon age calibration curve (0–55 cal kBP). Radiocarbon 62, 725–757.

- Rodbell, D., Hatfield, R., Abbott, M., Chen, C., Woods, A., Stoner, J., McGee, D., Tapia, P., Bush, M., Valero-Garcés, B., 2022. 700,000 years of tropical Andean glaciation. Nature 607, 301–306.
- Roosevelt, A.C., 2013. The Amazon and the Anthropocene: 13,000 years of human influence in a tropical rainforest. Anthropocene 4, 69–87.
- Rozas-Davila, A., Valencia, B.G., Bush, M.B., 2016. The functional extinction of Andean megafauna. Ecology 97, 2533–2539.
- Sanford Jr, R.L., Saldarriaga, J., Clark, K.E., Uhl, C., Herrera, R., 1985. Amazon rainforest fires. Science 227, 53–55.
- Seltzer, G.O., Rodbell, D., Baker, P., Fritz, S.C., Tapia, P., Rowe, H., Dunbar, R., 2002. Early warming of tropical South America at the last glacial-interglacial transition. Science 296, 1685–1686.
- Sombroek, W., 2001. Spatial and temporal patterns of Amazon rainfall. AMBIO A J. Hum. Environ. 30, 388–396.
- Stockmarr, J., 1971. Tables with spores used in absolute pollen analysis. Pollen Spores 13, 615–621.
- Stríkis, N.M., Cruz, F.W., Barreto, E.A., Naughton, F., Vuille, M., Cheng, H., Voelker, A. H., Zhang, H., Karmann, I., Edwards, R.L., 2018. South American monsoon response to iceberg discharge in the North Atlantic. Proc. Natl. Acad. Sci. USA 115, 3788-3703
- Urrego, D.H., Bush, M.B., Silman, M.R., Correa-Metrio, A.Y., Ledru, M.-P., Mayle, F.E., Paduano, G., Valencia, B.G., 2009. Millennial-scale ecological changes in tropical South America since the last glacial maximum. Past climate variability in South America and surrounding regions: from the Last Glacial Maximum to the Holocene 283–300. Springer.
- Urrego, D.H., Hooghiemstra, H., Rama-Corredor, O., Martrat, B., Grimalt, J., Thompson, L., 2015. Rapid millennial-scale vegetation changes in the tropical Andes. Clim. Past Discuss 11.
- Urrego, D.H., Silman, M.R., Bush, M.B., 2005. The Last Glacial Maximum: stability and change in a western Amazonian cloud forest. J. Quat. Sci.: Published for the Quaternary Research Association 20, 693–701.
- Van Breukelen, M., Vonhof, H., Hellstrom, J., Wester, W., Kroon, D., 2008. Fossil dripwater in stalagmites reveals Holocene temperature and rainfall variation in Amazonia. Earth Planet Sci. Lett. 275 (1–2), 54–60.
- Van der Hammen, T., Absy, M.L., 1994. Amazonia during the last glacial. Palaeogeogr. Palaeoclimatol. Palaeoecol. 109, 247–261.
- Van Der Hammen, T., Hooghiemstra, H., 1995. The el Abra stadial, a Younger Dryas equivalent in Colombia. Quat. Sci. Rev. 14, 841–851.
- Wang, X., Edwards, R.L., Auler, A.S., Cheng, H., Kong, X., Wang, Y., Cruz, F.W., Dorale, J. A., Chiang, H.-W., 2017. Hydroclimate changes across the Amazon lowlands over the past 45,000 years. Nature 541, 204–207.
- Whitney, B.S., Mayle, F.E., Punyasena, S.W., Fitzpatrick, K.A., Burn, M.J., Guillen, R., Chavez, E., Mann, D., Pennington, R.T., Metcalfe, S.E., 2011. A 45 kyr palaeoclimate record from the lowland interior of tropical South America. Palaeogeogr. Palaeoclimatol. Palaeoecol. 307, 177–192.
- Wickham, H., Chang, W., Wickham, M.H., 2016. Package 'ggplot2'. Create elegant data visualisations using the grammar of graphics. Versiones 2, 1–189.
- Zhang, Y., Chiessi, C.M., Mulitza, S., Sawakuchi, A.O., Häggi, C., Zabel, M., Portilho-Ramos, R.C., Schefuß, E., Crivellari, S., Wefer, G., 2017. Different precipitation patterns across tropical South America during Heinrich and Dansgaard-Oeschger stadials, Ouat. Sci. Rev. 177, 1–9.